Annex 3.

Form of opening (renewal) for Project / Sub-project of LRIP

APPROVED
JINR DIRECTOR
_____ /
"____" _____ 202 г.

SCIENTIFIC AND TECHNICAL REASONING FOR THE OPENING / RENEWAL OF PROJECT/SUB-PROJECT OF LARGE RESEARCH INFRASTRUCTURE PROJECT IN RESEARCH AREA WITHIN THE TOPICAL PLAN FOR JINR RESEARCH

1. General information on the project/subproject of the large research infrastructure project (hereinafter LRIP)

1.1 Theme code / LRIP (for renewable themes) - *the theme code includes the opening date, the closing date is not given, as it is determined by the completion dates of the projects in the topic.*

02-0-1085-2009/2023

1.2 Project/sub-project of a MIP code (for renewed themes)

1.3 Laboratory

DLNP

1.4 Scientific field

Particle physics

1.5 The name of the Project/subproject of the LRIP

AMBER (NA66)

1.6 Project/ sub-project of the LRIP Leader(s)

A. Guskov

1.7 Project/sub-project of the LRIP Deputy Leader(s) (scientific supervisor of the project/sub-project of the LRIP)

-

2 Scientific rationale and organisational structure

2.1 Annotation

AMBER (Apparatus for Meson and Baryon Experimental Research) is a new fixed-target experimental facility at the M2 beam line of the CERN SPS It will provide the site for a great variety of comprehensive measurements to address fundamental issues of Quantum Chromodynamics, which are expected to

lead to significant improvements in the understanding of QCD as the present theory of strong interactions. The proposed measurements cover the range from lowest-Q^2 physics as the determination of the proton radius by elastic muon-proton scattering, over average-Q^2 reactions to study hadron spectroscopy, to high-Q^2 hadron-structure investigations using the Drell-Yan, charmonia and prompt-photon production hard processes. It continues the impressive and very successful chain of the experiments: EMC – NMS – SMC – COMPASS that enriched significantly our knowledge of internal structure and properties of hadrons.

2.2 Scientific justification (purpose, relevance and scientific novelty, methods and approaches, methodologies, expected results, risks)

Introduction

The first phase of the AMBER experiment, approved by CERN, consists of three measurements.

The aim of the first measurement is an independent precision determination of the electric mean-square charge radius of the proton using elastic muon-proton scattering. Such a measurement appears timely, since in spite of many years of intense activity the proton-radius puzzle remains unsolved up to now. Presently, a discrepancy as large as 5 standard deviations exists between the two most recent precision measurements: 0.841 ± 0.001 fm (*CREMA*) from line-splitting measurements in laser spectroscopy of muonic hydrogen and 0.879 ± 0.008 fm from elastic electron-proton scattering (*MAMI).* We propose to perform a one-year measurement using high-energy muons of the CERN M2 beam line, which will provide a new and completely independent result on the proton radius with a statistical accuracy of 0.01 fm and considerably smaller systematic uncertainty. Using muons instead of electrons is highly advantageous, as several experimental systematic effects and also theoretical (radiative) corrections are considerably smaller. The measurement will employ a time-projection chamber filled with pure hydrogen up to pressures of 20 bar, which serves at the same time as a target and as detector gas.

The main objective of the proposed Drell-Yan and J/ψ production measurement is to make a major step forward in the determination of the nearly unknown pion and kaon parton distribution functions (PDFs). The planned measurements will provide key benchmarks for testing the most recent predictions of fundamental non-perturbative QCD calculations, such as lattice QCD and Dyson-Schwinger Equations formalism. At medium and large values of Bjorken-*x*, a quantitative comparison between the pion and the kaon valence distributions is of utmost importance. At smaller values of Bjorken-*x*, improved knowledge of the onset of the sea and gluon distributions in the meson will help in explaining the differences between the gluon contents of pions, kaons and nucleons, and hopefully provide clues to understand the mechanism that generates the hadron masses. Furthermore, a comparison between cross sections for positive and negative meson beams is expected to provide stringent experimental constraints on the J/ψ production mechanism, as well as an alternative way of accessing both quark and gluon distributions in the incoming meson. In parallel to meson structure measurements, the availability of heavier nuclear targets in the setup will allow the study of nuclear effects such as nuclear PDFs and partonic energy loss.

The purpose of the third measurement is the determination of the antiproton production cross section on proton and *He-4* targets for projectile energies from several ten to a few hundred GeV. In combination with similar measurements by LHCb in the TeV range, our data will provide a fundamental data set that will greatly improve the accuracy of the predicted natural flux of antiprotons in the galactic cosmic rays. This is of great importance as the indirect detection of Dark Matter (DM) is based on the search for products of DM annihilation or decay,

which are expected to appear as distortions in the spectra of rare Cosmic Ray components like positrons or antiprotons.

Project also includes preparation of the second phase of the experiment that includes the study of kaon structure and properties at wide range of Q^2 using RF-separated high-intensity kaon beam.

Physic case

The dynamical emergence of the large proton mass-scale ~1 GeV is one of the most striking features of the Standard Model. Its value is correlated with the size of the proton and hence with attempts to explain the confinement of gluons and quarks. Today there is a puzzle over that size: elastic electron scattering experiments and laser spectroscopy studies are in marked disagreement. In elastic lepton-nucleon scattering, the slope of the electric form factor G_E is measured at small values of Q^2. In laser spectroscopy, the Lamb shift is measured in electronic or muonic atoms. The numerous results published over the last decade are still contradicting, thereby constituting the so-called proton radius puzzle [1]. This discrepancy may point to physics beyond the Standard Model. In either case, solving the puzzle is crucial so that a hard mark is set for the value of the proton radius as a rigorous test of quantitative QCD; new experimental results are therefore of utmost priority.

To solve the puzzle, several new experiments were proposed and are still in preparation or already running: Prad in JLab [2,3], ELPH (RIKEN) [4], MAMI-A1 [5,6] and future MAGIX-MESA facility, (Mainz). In Fig. 1, a compilation of published results, sorted by time, and the accuracy expectation for the AMBER measurement are shown. So far, in scattering experiments the proton radius has only been studied with electrons. Measurements with muon beams are complementary and will test systematic effects such as those related. Besides AMBER, only the MUSE experiment at PSI [7] proposes to test the issue with muon beam. But it is optimised to test possible differences between electron-proton and muon-proton scattering in non-forward kinematics. The forward kinematics of the AMBER proposal greatly suppresses Coulomb-distortion effects, which at MUSE are of substantial size and have to be dealt with in the analysis. Altogether, the proposed measurement appears unique and complementary when compared to finished, ongoing and other planned experiments.

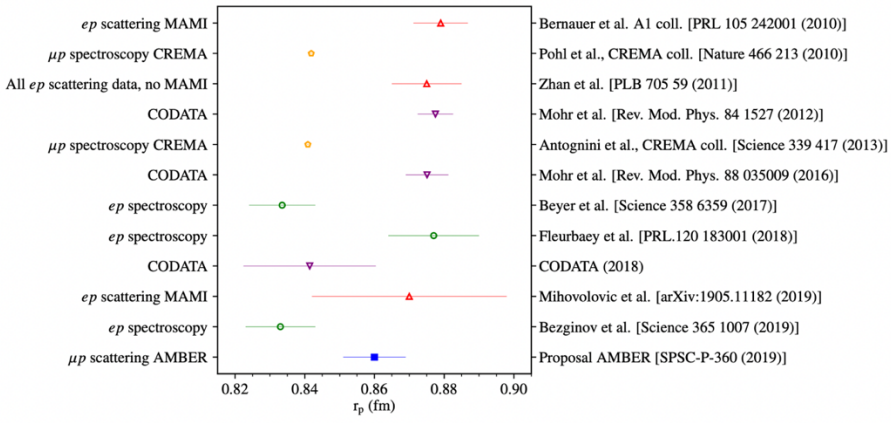

Fig 1. Compilation of data on the proton radius puzzle, sorted by time.

The quark-gluon structure of light mesons and the physical origin of their small masses are still largely unknown. While there are a lot of data available on the proton, the experimental determination of meson structure remains the long-awaited and critical input to theoretical efforts that seek to explain the emergence of massive composite hadrons, including the large mass difference between pion and proton. Two Standard Model mechanisms contribute to the

generation of mass. Spontaneous electroweak symmetry breaking gives rise to the Higgs mechanism providing fundamental particles with their current masses. Strong-interaction chiral symmetry breaking leads to the large masses of composite hadrons. In chiral QCD with massless quarks, hadron masses in the Lagrangian emerge through the trace anomaly of the energy-momentum tensor. For the proton, the binding energy and the mass of dressed quarks add to about 1 GeV. Very differently for the pion, the Goldstone Boson of the interaction, the binding energy and the dressed quark masses cancel each other [8]. In lattice QCD, the recently proposed Large Momentum Effective Theory (LaMET) [9] will make it possible to calculate quark and gluon distribution functions for hadrons quantitatively, see for example [10] and [11]. Such calculations greatly benefit from the arrival of Peta-scale supercomputers. Recently, there has been increasing interest in theoretical calculations of the parton structure of mesons, including the Nambu-Jona-Lasinio model [12,13], the chiral constituent quark model [14], the light-front constituent model [15], and from QCD Dyson-Schwinger equations [16,17].

Presently, all information about pion PDFs is extracted from rather uncertain pion-induced experiments made in 80-90th [18-21] and the results for leading neutrons production at HERA [22]. A new generation of experiments appears at the horizon. In the realm of DIS experiments, it was recently proposed to study the pion structure through final-state tagged DIS at JLab [23], while for preparing the long-range future the feasibility of pion and kaon-structure measurements at a future Electron-Ion Collider has been evaluated [24]. In the realm of Drell-Yan experiments, the existing high-intensity positive and negative pion beams, available for AMBER at CERN, provide already now a unique opportunity to study the structure of pions through pion-induced dimuon production off unpolarised nuclear targets.

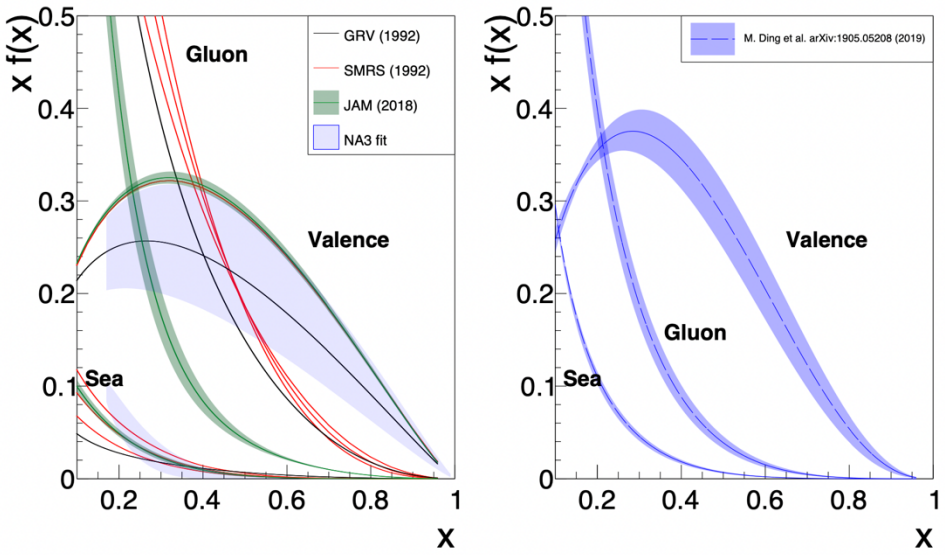

Fig. 2. Left: quark and gluon PDFs for the pion from global fits of GRV/S [19,20], SMRS [21], JAM [22] and the NA3 extraction [18]. Right: same but for the most recent calculation based on continuum analyses [25].

AMBER intends to perform separation of valence and sea-quark contributions in pion using combination of π^+/π^--induced data and to test the gluon content of the pion using such instruments as J/ψ and ψ' production in the gluon-gluon fusion hard subprocesses. The charmonia production mechanism is an additional topic to be studied in order to test such phenomenological models like ICEM, NRQCD etc. In parallel, possible flavour-dependent effects in nuclear targets will be investigated.

The indirect detection of Dark Matter is based on the search for the products of its annihilation or decay. They could appear as anomalies in the rare components of cosmic rays. In particular

cosmic-ray antimatter components, like antiprotons, antideuterons and positrons, promise to provide sensitivity to DM annihilation products on top of the standard astrophysical production. After the breakthrough from the satellite-borne PAMELA detector [26], the *p-bar* flux and the *p*-bar/*p* ratio have been measured with the unprecedented accuracy of a few percent by AMS-02 [27] in the energy range for a few GeV up to a few hundreds of GeV. In order to obtain a significant sensitivity to DM signals, it is then very important to keep a small uncertainty on the prediction of cosmic anti-proton produced in the collision with the interstellar medium (mainly p-p, p-He and He-He interactions). This uncertainty dominates in the range from 3 to 150 GeV as it is shown in Fig. 3.

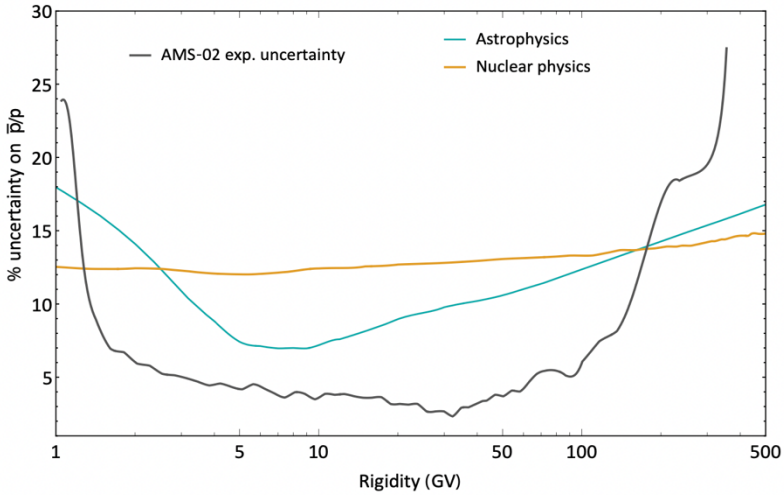

Fig. 3. Relative uncertainties afflicting the estimation for the *p*-bar/*p* ratio, shown as a function on the rigidity *p*/*Ze in comparison with the uncertainty of AMS-02 measurements.*

While for *p*+*p* collisions a few experimental datasets are available, the very first dataset on *p* + *He* collisions was collected at the end of 2015 by the LHCb experiment at 4 and 7 TeV. AMBER would contribute to this fundamental DM search by performing a complementary measurement with a proton beam of a few hundred GeV/c impinging on liquid hydrogen and liquid helium targets.

More details on the physics case could be found at the AMBER documents [28,29].

References

[1] Gil Paz, The Proton Radius Puzzle, Contribution to: DPF2019, e-Print: 1909.08108 (2019).
[2] A. Gasparian , M. Khandaker , H. Gao , D. Dipangkar, JLab Proposal E12-11-106.
[3] W. Xiong et al., A small proton charge radius from an electron–proton scattering experiment, Nature 575 (2019) 7781, 147-150.
[4] T. Suda, Electron scattering experiment off proton at ultra-low Q2 (2016).
[5] M. Mihovilovič et al, The proton charge radius extracted from the initial-state radiation experiment at MAMI, Eur. Phys. J. A 57 (2021) 3, 107.
[6] A. Vorobyev, Precision measurement of the proton charge radius in electron proton scattering, Phys. Part. Nucl. Lett. 16 (2019) 5, 524-529.
[7] R. Gilman et al, Studying the Proton "Radius" Puzzle with μp Elastic Scattering, e-Print: 1303.2160 [nucl-ex] (2013).
[8] C. D. Roberts, Perspective on the origin of hadron masses, Few Body Syst. 58 (2017) 1, 5.
[9] X. Ji, Parton Physics on a Euclidean Lattice, Phys. Rev. Lett. 110. (2013) 262002.
[10] Jian-Hui Zhang et al., Pion Distribution Amplitude from Lattice QCD, Phys. Rev. D 95. (2017) 9, 094514.
[11] A. Abdel-Rehim et al., Nucleon and pion structure with lattice QCD simulations at physical value of the pion mass Phys.Rev.D 92 (2015) 11, 114513.

[12] Seung-il Nam, Parton-distribution functions for the pion and kaon in the gauge-invariant nonlocal chiral-quark model, Phys.Rev.D 86 (2012) 074005.
[13] Parada T.P. Hutauruk, Valence-quark distributions of pions and kaons in a nuclear medium, Phys.Rev.D 100 (2019) 9, 094011.
[14] A. Watanabe, Meson cloud effects on the pion quark distribution function in the chiral constituent quark model, Phys.Rev.D 94 (2016) 11, 114008.
[15] B. Pasquini, Pion transverse momentum dependent parton distributions in a light-front constituent approach, and the Boer-Mulders effect in the pion-induced Drell-Yan process, Phys.Rev.D 90 (2014) 1, 014050.
[16] T. Nguyen et al, Pion and kaon valence-quark parton distribution functions, Phys.Rev.C 83 (2011) 062201.
[17] C. Chen et al, Valence-quark distribution functions in the kaon and pion, Phys.Rev.D 93 (2016) 7, 074021.
[18] J. Badier et al, Experimental Determination of the pi Meson Structure Functions by the Drell-Yan Mechanism, Z.Phys.C 18 (1983) 281.
[19] M. Gluck et al, Pionic parton distributions, Z.Phys.C 53 (1992) 651-656.
[20] M. Gluck et al, Pionic parton distributions revisited, Eur.Phys.J.C 10 (1999) 313-317.
[21] P.J. Sutton et al, Parton distributions for the pion extracted from Drell-Yan and prompt photon experiments, Phys.Rev.D 45 (1992) 2349-2359.
[22] P.C. Barry et al, First Monte Carlo Global QCD Analysis of Pion Parton Distributions, Phys.Rev.Lett. 121 (2018) 15, 152001.
[23] A. Camsonne, et al., Measurement of Tagged Deep Inelastic Scattering (TDIS), JLAB proposal C12-14-010.
[24] A. Accardi, et al., Electron Ion Collider: The Next QCD Frontier, Eur. Phys. J. A52 (9) (2016) 268.
[25] M. Ding et al., Symmetry, symmetry breaking, and pion parton distributions, Phys.Rev.D 101 (2020) 5, 054014.
[26] O. Adriani et al., Measurement of the flux of primary cosmic ray antiprotons with energies of 60 MeV to 350 GeV in the PAMELA experiment, JETP Lett. 96 (2013) 621-627, Pisma Zh.Eksp.Teor.Fiz. 96 (2012) 693-699.
[27] M. Aguilar et al., Antiproton Flux, Antiproton-to-Proton Flux Ratio, and Properties of Elementary Particle Fluxes in Primary Cosmic Rays Measured with the Alpha Magnetic Spectrometer on the International Space Station, Phys.Rev.Lett. 117 (2016) 9, 091103.
[28] B. Adams et al., Letter of Intent: A New QCD facility at the M2 beam line of the CERN SPS (COMPASS++/AMBER), e-Print: 1808.00848 (2018).
[29] B. Adams et al., Proposal for Measurements at the M2 beam line of the CERN SPS (Phase-1), CERN-SPSC-2019-022 / SPSC-P-360 (2019).

Proposed measurements

The AMBER experimental setup is based on the updated COMPASS spectrometer [1,2]. The setup can be divided into four parts along the beam axis. It starts with the beam line telescope and the detectors that identify the incoming beam particles. It is followed by the target region, which target zone will be modified for needs of the particular measurement. The third part called the Large Angle Spectrometer (LAS) is built around the first dipole magnet SM1. The fourth part is the Small Angle Spectrometer (SAS), which occupies the downstream part of the setup. Both, the LAS and the SAS include a hadron and electromagnetic calorimeter and the muon identification system.

The JINR group is responsible for upgrade and operation of the hadron calorimeter HCAL1 and the large-angle muon identification system MW1 (Muon Wall 1). It also participates together with a group from University of Turin in the production and support of the Bulk Micromegas tracking detectors which will replace the outdated probe chambers (MWPC) in the SAS downstream the SM2 magnet.

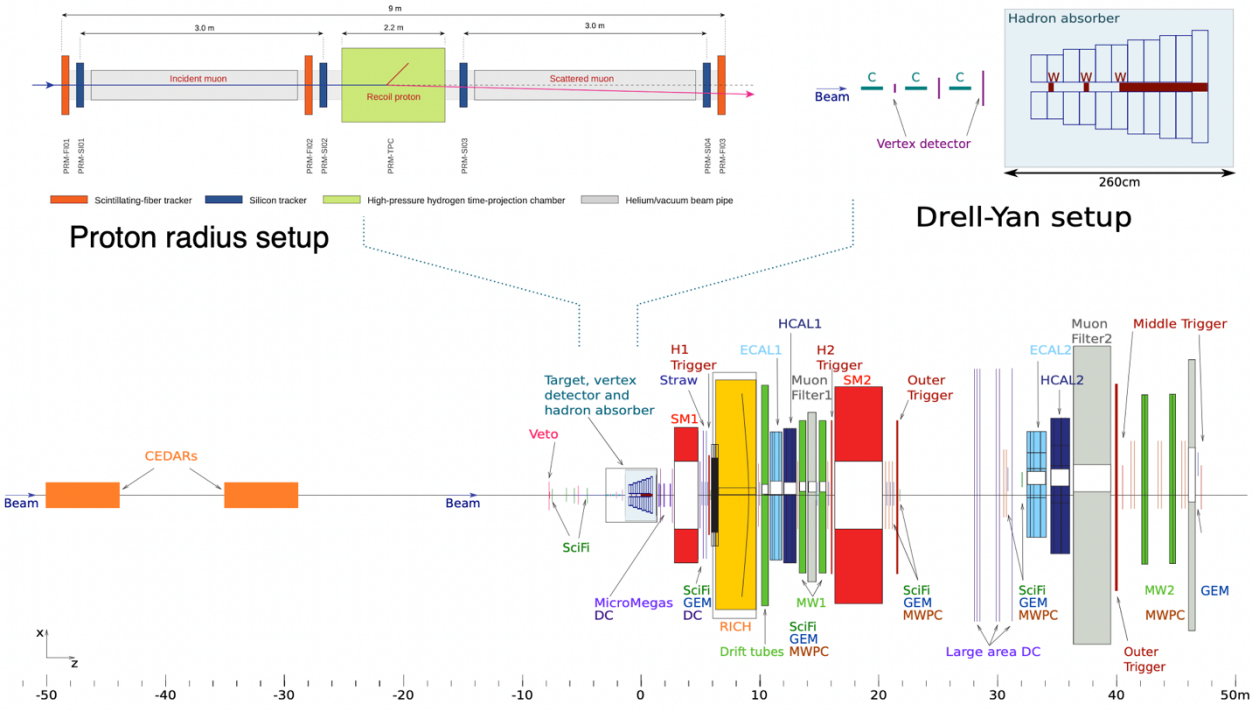

Fig. 4. General view of the AMBER setup. Target regions for the proton radius (left) and the Drell-Yan (right) measurements are enlarged.

The idea of the **proton radius determination** is based on the electric form factor $G_E(Q^2)$ slope measurement at $Q^2=0$:

$$\langle r_E^2 \rangle = -6\hbar^2 \left. \frac{\mathrm{d}G_E(Q^2)}{\mathrm{d}Q^2} \right|_{Q^2=0}$$

The form factor $G_E(Q^2)$ could be determined from cross section of elastic muon-proton scattering:

$$\frac{d\sigma}{dQ^2} = \frac{\pi\alpha^2}{Q^4 m_p^2 \vec{p}_\mu^{\,2}} \left[\left(G_E^2 + \tau G_M^2 \right) \frac{4E_\mu^2 m_p^2 - Q^2(s-m_\mu^2)}{1+\tau} - G_M^2 \frac{2m_\mu^2 Q^2 - Q^4}{2} \right]$$

$$= \frac{4\pi\alpha^2}{Q^4} R \left(\varepsilon G_E^2 + \tau G_M^2 \right),$$

where

$$R = \frac{\vec{p}_\mu^{\,2} - \tau(s - 2m_p^2(1+\tau))}{\vec{p}_\mu^{\,2}(1+\tau)}, \qquad \varepsilon = \frac{E_\mu^2 - \tau(s-m_\mu^2)}{\vec{p}_\mu^{\,2} - \tau(s-2m_p^2(1+\tau))}$$

are the recoil and longitudinal-polarization variables, respectively, $\tau=Q^2/(2m_p)^2$ and s is the scenter-of mass energy. At the small values of Q^2 (*i.e.* small τ), the contribution from *the magnetic form factor $G_M(Q^2)$ is small and could be taken into account* by assuming some shape for G_M, so that only G_E is left as a free parameter. Such approach introduces an uncertainty for the G_E measurement much below 0.1%.

AMBER proposes to measure elastic muon-proton scattering using a 100 GeV muon beam and a pressurised hydrogen gas target. For a precise measurement of the proton radius, the relevant momentum transfer region is $0.001 < Q^2/(\mathrm{GeV}^2/c^2) < 0.04$, which requires to operate the target as a TPC in order to detect the track of the recoil proton. The scattered muon will be

measured with the spectrometer. The silicon telescopes surrounding the TPC will be used for measuring the muon scattering angle with high accuracy. The pressure of the gas will be optimised for having, on the one hand, sufficiently low stopping power such that a proton recoil track is detectable, and on the other hand it still stops in the TPC volume. In addition, the electromagnetic calorimeter detect the (rare) radiative events, by which soft photons with energies up to 2 GeV are emitted. Muon identification is performed using muon filter and hodoscopes. Since triggering only on the proton recoil would imply Q^2-dependent efficiency variations that could not be controlled using the data themselves, a trigger component from the muon trajectory has to be added. The beam rate is too high to record all events, the beam trigger will have to be extended by a new component that allows to veto muons with a scattering angle below about 5 μrad. A continuous read-out is planned to solve current issues of rate capability and will allow for implementing the above described event selection in an elegant and efficient manner.

Two years of data taking is planning to collect data with different TPC pressure and both signs and different momenta of the muon beam to estimate systematics (see Tab. 1). In order to achieve a statistical uncertainty of the measurement below 1% at least 50 million events in the relevant Q^2 range have to be collected. As for the systematics, the main contributions for the bin-to-bin measurement of the cross-section shape of muon-proton scattering are presented in Tab. 2 and the total value should be below 0.6%. So, the total uncertainty of the proton radius measurement by AMBER could be reduced to about 0.01 fm.

Tab 1. Settings proposed for the proton radius measurement.

Beam setting	**TPC pressure setting**	**Duration**	**Purpose**
μ^+, 100 GeV	20 bars	92 days	$2.5 < Q^2/(10^{-3}\text{GeV}^2) < 40.0$
μ^+, 100 GeV	4 bars	67 days	$1.0 < Q^2/(10^{-3}\text{GeV}^2) < 8.0$
μ^-, 100 GeV	4 bars	67 days	control of charge dependence
μ^+, 60 GeV	4 bars	34 days	control of energy dependence

Tab 2. Expected systematic uncertainties of the cross-section shape measurement.

uncertainty source	**estimate in %**
Monte-Carlo acceptance correction	0.2
Q^2 resp. beam energy calibration	0.2
radiative corrections	0.1
fitting procedure	0.1
(linear) sum	<0.6

The pion-induced Drell-Yan process ($\pi p \rightarrow \mu^+\mu^- X$) with $M_{\mu\mu}$>4.3 GeV will be used for ***the sea-valence quarks separation*** *in the pion.* The valence quarks in pion are defined as:

$$u_{val}^{\pi^+} = u^{\pi^+} - \bar{u}^{\pi^+} \quad \text{and} \quad d_{val}^{\pi^-} = d^{\pi^-} - \bar{d}^{\pi^-}$$

Assuming charge and the SU2 symmetry: $u_{val}^{\pi^+} = \bar{d}_{val}^{\pi^+} = \bar{u}_{val}^{\pi^-} = d_{val}^{\pi^-}$

Additionally, SU(3) flavour-symmetry is assumed for the sea quarks in the pion:

$$\bar{u}_{sea}^{\pi} = u_{sea}^{\pi} = \bar{d}_{sea}^{\pi} = d_{sea}^{\pi} = \bar{s}_{sea}^{\pi} = s_{sea}^{\pi}$$

So, having an isoscalar target (D), it is possible to build the two linear combinations of pion-induced Drell-Yan cross section:

$$\Sigma_{val}^{\pi D} = -\sigma^{\pi^+ D} + \sigma^{\pi^- D} \quad \text{and} \quad \Sigma_{sea}^{\pi D} = 4\sigma^{\pi^+ D} - \sigma^{\pi^- D} \ ,$$

where the first combination contains only valence-valence terms, while the second one comprises only sea- valence and valence-sea terms.

The gluon-gluon fusion and q-qbar annihilation are two main hard processes contributing to the J/ψ production. A comparison of the different models to the measured x_F distribution in different transverse momentum (p_T) regions and the J/ψ polarization (also as a function of x_F) will represent a thorough test of the theory of quarkonium production in the low-p_T domain. This addresses, on the one hand, the factorization ansatz and gluon PDFs and, on the other hand, the two hadronization models with their (possibly different) predictions for the q-q-bar and g-g contributions to the J/ψ yield. This goal can be achieved with a high-statistics measurement, sensitive to the shape differences between the q-q and g-g x_F-differential cross sections and to the differences between the corresponding decay angular distributions.

Positive and negative hadron beams will be scattered off the segmented carbon target where the elements will be separated by the vertex detector. Two Cherenkov threshold detectors, CEDARs, will be responsible for the pion identification. Precise silicon detectors will define beam tracks. The alumina/stainless steel hadron absorber with a tungsten plug has to stop all the hadrons downstream the target in order to reduce the background from the leptonic decays of pions and kaons. Two additional tungsten targets for study of the nuclear effects will be installed in the hole of the absorber. The Drell-Yan events will be triggered by the hodoscope-based trigger and muon momenta will be reconstructed in both the LAS and the SAS. The expected dimuon mass resolution is 115 MeV for the J/ψ peak. For 2 years of data taking, 213 days with positive (1.7×10^7 part./s) and 67 days with negative (6.8×10^7 part./s) AMBER will collect 21.7×10^3 and 67.0×10^3 Drell-Yan events for the mass range 4.3-8.5 GeV, respectively, for the main carbon target. This is about one order of magnitude higher than the statistics of any previous experiments with isoscalar target.

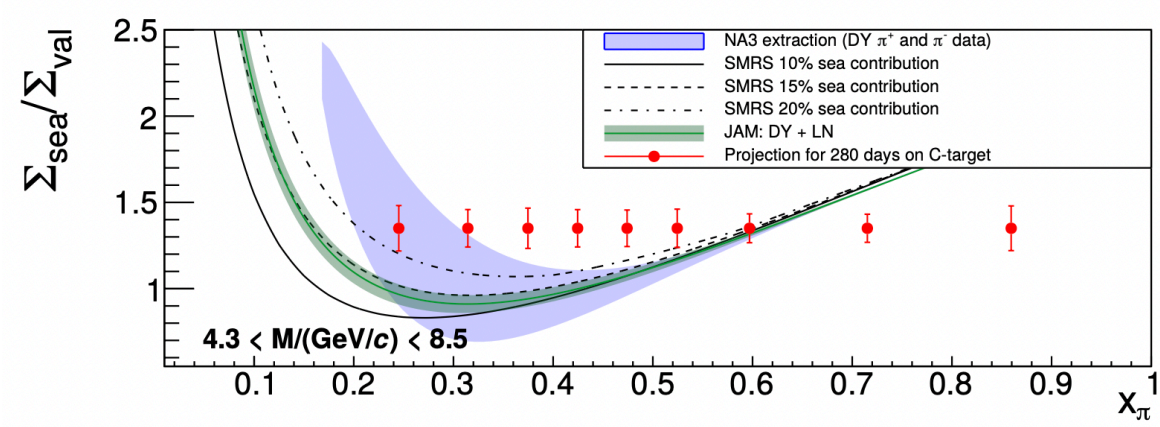

Fig. 5. Ratio $\sum_{sea}/\sum_{val}$. as a function of x_π, using three different sea-quark distributions and the expected statistical errors.

The corresponding statistics for the J/ψ muonic decays is 1.2×10^6 and 1.8×10^6 events. Comparable statistics will also be collected with protons. Additional, 2.5 times smaller statistics will be collected for the tungsten targets. Estimations for the accuracies of the separation of the valence/sea contributions for the Drell-Yan process, measurement of the differential cross sections $d\sigma/dx_F$ for the J/ψ production and the J/ψ polarization in the Collins-Soper reference frame are presented in Figs. 5, 6(left) and 6(right), respectively.

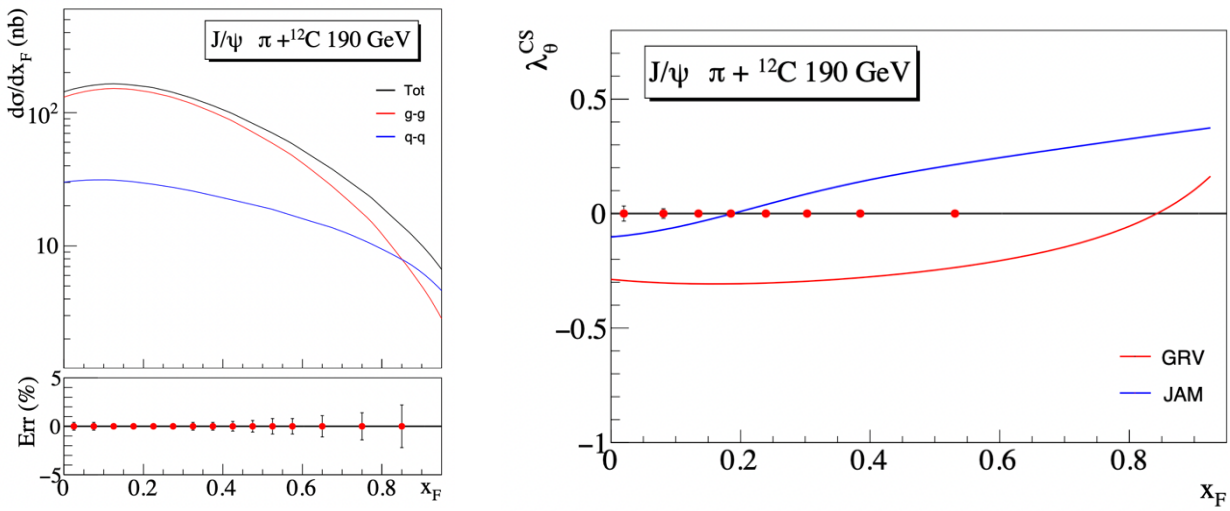

Fig. 6. (left) Pion-induced J/ψ cross section prediction for a carbon target computed with the ICEM model (black line). The red and blue lines show the *qq*bar and gg contributions, respectively. Estimated relative uncertainties of the proposed measurement are presented below. (right) Pion-induced J/ψ polarisation as a function of x_F *calculated within the ICEM framework for different sets of pion PDFs.* Statistical accuracy achievable with the experimental assumptions is also shown.

The main sources of the systematic uncertainties are: i) flux determination, ii) beam particle identification, iii) secondary interaction (the fraction of such DY events in carbon target could reach 5%), iv) trigger efficiency estimation, v) nuclear effects. Nevertheless, the systematic uncertainty of the proposed Drell-Yan and charmonia measurements is expected to be much smaller than the estimated statistical uncertainty.

Secondary positive hadron beam of 50, 100, 150, 200 and 280 GeV/c extracted to a liquid hydrogean and liquid helium targets is planned to be used for the measurement of the **anti-proton production cross section measurement**. The CEDAR detectors will be used to identify beam protons. AMBER plans to measure this cross section as a double-differential one in the momentum and forward angle of the *pbar*. The spectrometer will track the secondary charged particles and measure their momentum, while their velocity will be measured by the RICH detector that will allow for particle identification and in particular for anti-proton selection. For the momentum range 18-45 GeV/c, RICH will identify the antiprotons by their mass, and in the range 10-18 GeV /c, the absence of the RICH signal, *i.e.* the veto mode, will be used to identify the particle as not π or not *K*.

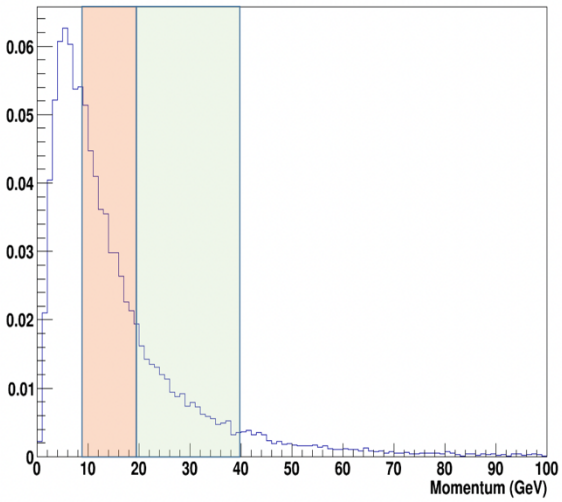

Fig. 7. Expected *antiproton* momentum spectrum for 190 GeV. The orange range corresponds to the antiproton identification in the veto mode while the green range shows the normal identification mode.

Considering a measurement of the double-differential cross section with 10 bins in momentum and pseudorapidity each, a statistical uncertainty of ≈ 0.5% per data point will be reached in 1 day of beam time. The statistical error is only a small contribution to the total error. Several corrections to the event and trigger counts are needed to obtain an accurate measurement. Each of these corrections contributes to the systematic uncertainty. Some of these factors have already been studied for the COMPASS hadron program. Finally, a total systematic uncertainty is estimated to be not exceeding 5%.

As for the running plans, a short test run is already performed in 2022. It will be followed by the main period of data taking.

Hardware responsibility of the JINR group

The Muon Wall 1 (MW1) system provides scattered muon identification capability in the LAS and is one of the most important detector especially for the Drell-Yan program. The system consists of two stations separated by a 60 cm thick iron absorber. Each station has four detectors with two planes on both sides, based on Mini Drift Tubes working in the proportional mode. Vertical and horizontal tubes provide the X and Y coordinates. The detectors have spatial resolution 3 mm and the efficiency of about 90% that is close to their geometrical efficiency. Drift time in the Ar/CO^2 is below 150 ns. The front-end part pf the detector should be upgraded to provide compatibility with the new DAQ system.

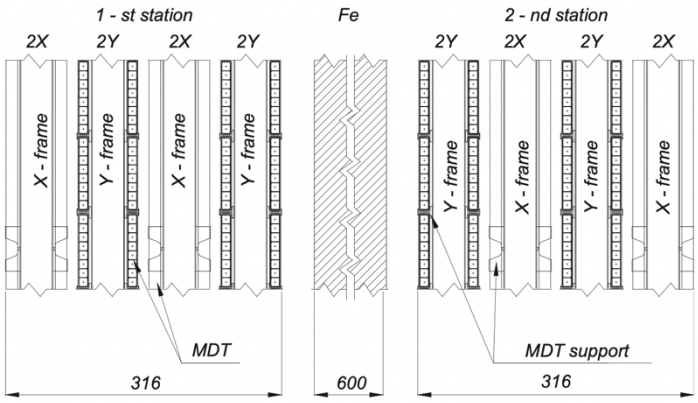

Fig. 8, Schematic layout of the MW1

The hadron calorimeter 1 (HCAL1) is placed before the MW1. HCAL1 has a modular structure, each module consisting of 40 layers of iron and scintillator plates, 20 and 5mm thick, respectively, amounting to 4.8 nuclear interaction lengths. It has the energy resolution of about $50\%/\sqrt{E} \oplus 8\%$ and provides hadron muon identification in the range from 5 to 100 GeV. The electronic part of the detector should also be re-

The Bulk Micromegas detectors will be constructed at JINR in close collaboration with the University of Turin (electronic part) in order to provide tracking capabilities in the SAS. They should have an active arear of 15 m^2 (3 chambers with 3 layers X,Y,V) and provide spatial resolution on the level of 1 mm. The prototype of such chamber was produced at JINR and tested in 2021.

References

[1] P. Abbon et al., The COMPASS experiment at CERN, NIM. A 577 (2007) 455-518.
[2] P. Abbon et al., The COMPASS Setup for Physics with Hadron Beams, NIM A 779 (2015) 69-115

The main risk to the project's implementation is the complication of the geopolitical situation and the termination of JINR's participation in the works of CERN.

2.3 Estimated completion date

2030

2.4 Participating JINR laboratories

DLNP, VBLHEP, LIT

2.4.1 MICC resource requirements

Computing resources	Distribution by year				
	1st year	2nd year	3rd year	4th year	5th year
Data storage (TB) - EOS - Ribbons	-	-	-	-	-
Tier 1 (core-hour)	-	-	-	-	-
Tier 2 (core-hour)	-	-	-	-	-
SC Talker (core-hour) - CPU - GPU	-	-	-	-	-
Clouds (CPU cores)	-	-	-	-	-

2.5. Participating countries, scientific and educational organisations

Organisation	Country	City	Participants	Type of agreement
Albert Ludwigs Universitaet	**Germany**	Freiburg	**H. FISCHER +3**	**MoU**
Czech Technical University in Prague	Czechia	Prague	J. NOVY +11	MoU
Charles University	Czechia	Prague	J. MATOUSEK+5	MoU
University of Bonn	Germany	Bonn	B. KETZER +10	MoU
Institute for High Energy Physics	Russia	Protvino	S. DONSKOV +1	MoU
Institute of Experimental Physics	Poland	Warsaw	B. BADELEK	MoU
Laboratorio de Instrumentação e Física Experimental de Partículas	Portugal	Lisbon	C. QUINTANS+2	MoU
Los Alamos National Laboratory	USA	Los Alamos	L. BAUDINO	MoU
NRC Kurchatov Institute PNPI	Russia	Gatchina	A. DZUBA +5	MoU
National Centre for Nuclear Research	Poland	Warsaw	A. SANDACZ +1	MoU
Lebedev Institute of Physics	Russia	Moscow	M. ZAVERTYAEV +1	MoU
School of Physics and Astronomy	UK	Glazgow	B. SEITZ +1	MoU
Technische Universitaet Muenchen	Germany	Munchen	S. PAUL +7	MoU
Tel Aviv University	Israel	Tel Aviv	J. LICHTENSTADT	MoU
Trento Institute for Fundamental Physics and Applications	Italy	Trento	P. ZUCCON + 3	MoU
Universita e INFN Torino	Italy	Turin	D. PANZIERI +3	MoU
Universita e INFN Trieste	Italy	Trieste	A. MARTIN +4	MoU
University of Aviero	Portugal	Aviero	C. AZEVEDO +1	MoU
Yamagata University	Japan	Yamagata	J. HIRUMA	MoU
Warsaw University of Technology	Poland	Warsaw	R. KURJATA	MoU

2.6. Co-executing organisations *(those collaborating organisations/partners without whose financial, infrastructural participation the implementation of the research programme is impossible. An example is JINR's participation in the LHC experiments at CERN).*

CERN

3. Staffing

3.1. Staffing needs in the first year of implementation

№№ n/a	**Category employee**	**Core staff, Amount of FTE**	**Associated Personnel Amount of FTE**
1.	scientific staff	8	
2.	engineers	2	
3.	professionals	2	
4.	employees		
5.	workers		
	Total:	**12**	**0**

3.2. Human resources available
3.2.1. JINR core staff

№№ п/а	Category of employees	NAME	Division	Position	Amount of FTE
1.	scientific staff	Alexeev G.D.	DLNP	Head of sector	0.5
2.		Denisenko I.I.	DLNP	Head of sector	0.1
3.		Frolov V.N.	DLNP	Researcher	0.5
4.		Gavrischuk O.P.	VBLHEP	Leading researcher	0.5
5.		Gongadze A.	DLNP	Head of sector	0.3
6.		Gridin A.O.	DLNP	Researcher	0.6
7.		Guskov A.V.	DLNP	Head of department	0.3
8.		Gushterski R.	VBLHEP	Researcher	1.0
9.		Korzenev A.Yu.	VBLHEP	Leading researcher	0.1
10.		Maltsev A.	DLNP	Junior researcher	0.8
11.		Peshekhonov D.V.	VBLHEP	Head of branch	0.2
12.		Savin I.A.	VBLHEP	Director emeritus	0.5
13.		Zemlyanichkina E.V.	VBLHEP	Head of sector	0.7
14.		Zhuravlev N.I.	DLNP	Senior researcher	0.5
15.		Abazov V.M.	DLNP	Researcher	0.5
16.		Tokmenin V.V.	DLNP	Researcher	0.5
17.		Piskun A.A.	DLNP	Junior researcher	0.5
18.		Selyunin A.S	DLNP	Junior researcher	0.1
19.		Anfimov N. V.	DLNP	Head of sector	0.1
20.	engineers	Anosov V.A.	VBLHEP	Leading engineer	0.3
21.		Shunko A.A.	VBLHEP	Engineer-constr., 1 cat	0.5
22.		Koviazina N.A.	DLNP	Engineer	0.5
23.		Samartsev A.G.	DLNP	Engineer-constr., 1 cat	0.5
24.	professionals	Petrosyan A. Sh.	LIT	Leading programmer	0.3
25.		Vtyurin A.V.	DLNP	Research assistant	1.0
26.		Seryubin S.S.	DLNP	Research assistant	0.5
	workers				
	Total:	**26**			**11.9**

3.2.2. JINR associated personnel

№№ п/а	Category of employees	Partner organisation	Amount of FTE
1.	Scientific employees		
2.	engineers		
3.	professionals		
4.	workers		
	Total:	**0**	**0**

4. Financial support

4.1 Total estimated cost of the project/sub-project of the LRIP

Forecast of the total estimated cost (specify cumulatively for the whole period, excluding FPC). The details are given in a separate form.

590 000 $ for 3-year period

4.2 Extrabudgetary funding sources

Estimated funding from co-executors/customers - total.

Project (sub-project of the LRIP) Leader _____/_____/

Date of submission of the project (sub-project of the LRIP) to DSOA: _____
Date of decision of the laboratory's STC: _____ document number: _____

Year of the project (subproject of the LRIP) opening: _____

(for renewable projects) -- Project start year: _____

Schedule proposal and resources required for the implementation of the Project / Sub-project of the LRIP

Names of costs, resources, sources of funding			Cost (thousands of dollars) resource requirements	Cost, distribution by year				
				1st year	2nd year	3rd year	4th year	5th year
		International cooperation (IC)	300	90	120	90		
		Materials	90	30	30	30		
		Equipment and third-party services (commissioning)	200	80	80	40		
		Commissioning work						
		Services of research organisations						
		Acquisition of software						
		Design/construction						
		Service costs (*planned in case of direct project affiliation)*						
Resources required	**Normo-hours**	Resources						
		– the amount of FTE,	34	12	10	12		
		– accelerator/installation,						
		– reactor,….						
Sources of funding	**Budgetary resources**	JINR budget *(budget items)*	590	200	230	160		
	Extrabudgetary (supplementary estimates)	Contributions by co-contractors Funds under contracts with customers Other sources of funding						

Project (sub-project of the LRIP) Leader_____/_____/

Laboratory Economist _____/_____/

APPROVAL SHEET FOR PROJECT / SUBPROJECT OF THE LRIP

NAME OF THE PROJECT/SUBPROJECT OF THE LRIP

DESIGNATION OF THE PROJECT / SUBPROJECT OF THE LRIP

PROJECT/SUBPROJECT OF THE LRIP CODE

THEME / LRIP CODE

NAME OF THE PROJECT/ SUBPROJECT OF THE MIP LEADER

AGREED
JINR VICE-DIRECTOR

SIGNATURE	NAME	DATE

CHIEF SCIENTIFIC SECRETARY

SIGNATURE	NAME	DATE

CHIEF ENGINEER

SIGNATURE	NAME	DATE

LABORATORY DIRECTOR

SIGNATURE	NAME	DATE

CHIEF LABORATORY ENGINEER

SIGNATURE	NAME	DATE

LABORATORY SCIENTIFIC SECRETARY
THEME / MIP LEADER

SIGNATURE	NAME	DATE

PROJECT / SUBPROJECT OF THE LRIP
LEADER

SIGNATURE	NAME	DATE

APPROVED BY THE PAC

SIGNATURE	NAME	DATE